Performance Comparison of a Hybrid Dual-Tuned $^{23}Na/^{1}H$ Birdcage to a Single-Tuned ^{23}Na Birdcage with Identical Geometry

B. Peterson[1], R. Watkins[2], G. Morrell[3], S. Allen[4], D. Park[1], J. Kaggie[5], G. E. Gold[2], and N. K. Bangerter[1]

[1]Department of Electrical & Computer Engineering, Brigham Young University, Provo, Utah, United States, [2]Department of Radiology, Stanford University, Stanford, California, United States, [3]Department of Radiology, University of Utah, Salt Lake City, Utah, United States, [4]Department of Physics, Brigham Young University, Provo, Utah, United States, [5]Department of Physics, University of Utah, Salt Lake City, Utah, United States

INTRODUCTION: Recent improvements in coil and gradient hardware, the availability of whole-body scanners with high polarizing field strengths, and the development of efficient pulse sequences with extremely short echo times have made feasible sodium MRI *in vivo* in reasonable scan times. These advances have rekindled interest in sodium MRI over the past decade for a variety of applications, including the assessment of cartilage health [1], characterization of tumors [2], detection of abnormal sodium levels in the kidneys [3], and assessment of tissue damage following stroke [4].

Dual-tuned $^{1}H/^{23}Na$ coil configurations (i.e., coils that resonate at both sodium and hydrogen frequencies) are highly desirable for many applications of sodium MRI. Sodium image acquisition can then be performed in conjunction with a standard ^{1}H exam without the need to move the patient to change coils. This is particularly advantageous when accurate registration of sodium and proton images is required.

Many dual-tuned coil designs employ frequency block traps, allowing selective routing of different frequencies through either spate rungs or rings in a birdcage structure. This approach suffers from significant inductive losses (due to wire resistance in the inductor) and magnetic field losses (due to inductors coupling to other structures or radiating in air), lowering coil electrical Q and SNR performance [5].

This work is based on a hybrid low-pass ^{23}Na, high-pass ^{1}H birdcage design (described by our collaborators at Stanford in a separate abstract) that employs multiple end rings in a single birdcage structure to make it dual resonant without frequency block traps [6]. The design incorporates a short *z*-FOV sodium quad low-pass birdcage in the central section of a split *z*-axis proton quad high-pass birdcage. High-pass birdcage coils are in general symmetric about the *z*-axis, with balanced currents in opposite directions such that the addition of a ring at the *z*-axis center has no significant effect.

In this study, we compare the sodium performance (SNR and B1 homogeneity) of the hybrid dual-resonant design to that of a single-tuned quadrature sodium birdcage coil with identical geometry to the sodium quadrature low-pass birdcage in the central section of the dual-resonant coil. Our results indicate that the sodium performance degradation of the dual-tuned design relative to the single-tuned sodium birdcage geometry is minimal.

METHODS: A hybrid low-pass sodium, high-pass hydrogen dual-resonant quadrature birdcage (Figure 1a) was built and tuned for both sodium and hydrogen imaging at 3T. Geometry of this dual-resonant birdcage was: inside diameter = 16 cm, inner end-ring separation (low-pass sodium) = 8.4 cm, outer end-ring separation (high-pass hydrogen) = 24.5 cm. A single-tuned low-pass sodium quadrature birdcage (Figure 1b) was then constructed with identical geometry to the inner (sodium) portion of the dual-resonant structure (inside diameter = 16 cm, end-ring separation = 8.4 cm), and tuned for sodium imaging at 3T.

A uniform cylindrical phantom with [Na+] of 150 mM was constructed to fit inside the coils. 3D sodium images of the phantom were then acquired (both magnitude images and B1 maps) with each coil using a custom EPI GRE sequence adapted for phase-sensitive sodium B1 mapping [7].

A region of interest was defined across a central portion of the phantom, and SNR measured across the ROI in sodium images from each coil. The standard deviation of the B1 map values across the sensitive region of the coils was also measured for each coil to give a measure of B1 homogeneity.

RESULTS AND DISCUSSION: Sodium magnitude images for a central slice through the phantom for each coil are shown in Figure 2, along with the measured SNR across the central region of interest. An SNR loss of less than 3% is observed in the dual-resonant structure relative to the single-resonant birdcage. B1 maps for a central slice are shown for each coil in Figure 3. While there are some variations in the B1 maps between coils and the sensitive volume is apparently slightly smaller in the single-tuned design, the dual-resonant structure is only slightly less homogeneous for sodium than the single-tuned coil. Overall, dual-resonance is achieved in this hybrid design with remarkably little performance penalty for sodium imaging relative to a single-tuned sodium birdcage design. Future work will assess the performance of the ^{1}H high-pass portion of the hybrid dual-resonant coil.

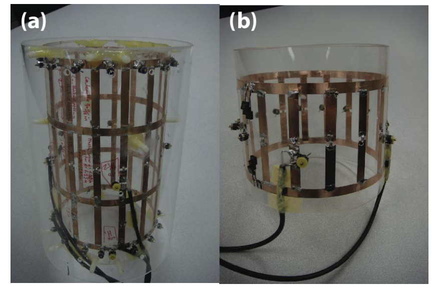

Figure 1: (a) Hybrid low-pass ^{23}Na, high-pass ^{1}H dual-resonant dual-quadrature coil, and (b) single-tuned low-pass ^{23}Na quadrature birdcage with identical geometry to sodium (low-pass) section of dual-resonant design.

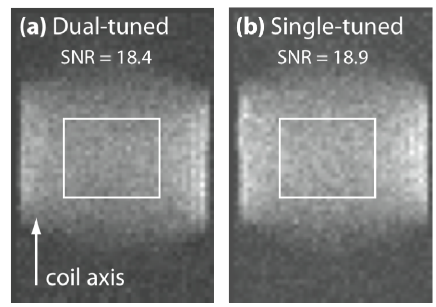

Figure 2: Magnitude sodium images, with SNR measurements across the indicated ROI. The dual-tuned design achieves nearly the same SNR performance as the single-tuned design.

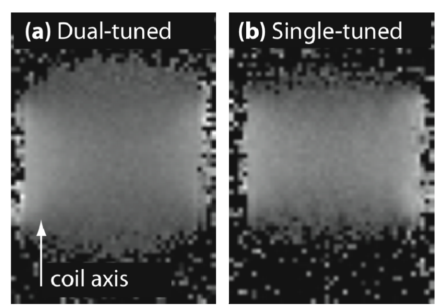

Figure 3: Sodium B1 maps (acquired with a phase-sensitive sodium EPI B1 mapping technique). Both coil designs achieve very good B1 homogeneity across the sensitive volume.

REFERENCES:

[1] Shapiro et al., Magn Reson Med. 2002; 47:284.
[2] Ouwerkerk et al., Radiology 2003; 227:529.
[3] Maril et al., Magn Reson Med 2006; 56:1229.
[4] Thulborn et al., Neuroimaging Clin N Am. 2005; 15:639.
[5] Shen et al., Magn Reson Med 1997; 38:717
[6] Derby et al., J Magn Reson Imaging 1990; 86:645
[7] Morrell et al., Magn Reson Med 2008; 60(4):889-894.